Eliminating the Inconsistencies in the Li-O_2 Cell Production Process

Connor Smyth

Registration Number: 140127946

Supervisor: Dr Anthony Rennie

Date: 27/03/2015

Keywords: Li-O2 Battery, Inconsistencies, Lithium Anode, Activated Carbon Cathode

Abstract

Due to the exceptionally high theoretical specific energy of the optimum Li-O_2 cell (3505 Wh/kg), research into this battery chemistry is at an all-time high. This has identified numerous problems for the technology as these cells suffer from poor rechargeability and can be massively inconsistent. Therefore, this study aimed to produce a batch of consistent cells for future characterisation.

13 Swagelok cells were produced with a solid lithium anode, an activated carbon cathode and 1M $LiPF_6$ in TEGDME electrolyte solution. Consistency was determined via the standard deviation of the specific energies (Wh/kg) during galvanostatic charge and discharge cycling.

The data produced reiterated that Li-O2 cells are inconsistent but demonstrated that through the act of repetition inconsistencies could be significantly reduced. This study therefore recommends that the experiment be repeated with a larger sample size to reduce the standard deviation. Further investigation is also needed to identify the cause of the inconsistency.

Contents

1 Introduction

Due to an increased awareness of the risks involved with continuing to perpetuate a fossil fuel economy there is now a strong drive from society to enter into a low-carbon economy. This drive has highlighted energy storage as one of the means to achieve this.

Energy storage is now considered to be essential for the ongoing development and the future of the energy industry within the UK. It will play an integral role in implementing renewables, decentralising energy production, encouraging and supporting demand side management and powering electric vehicles. As a result of a successful implementation of various energy storage technologies, the UK could reduce its reliance on fossil fuels which will consequently result in improved energy security and a greener reputation. International relations could also be strengthened through large-scale, cooperative storage mechanisms which reiterates the potential importance of energy storage.

The method of energy storage explored throughout this report are Lithium-Oxygen (Li-O_2) batteries, a type of metal-air battery. As with all batteries they are suitable for a range of applications and even though they are considered to be a relatively immature technology their potential strengths over other battery chemistries are clear. The theoretical, maximum potential energy of Li-O_2 batteries is significantly higher than the already commercially successful Li ion battery which is the reasoning behind research in this area (see Table 1).

Table 1 - Comparison of theoretical energy maximums for different battery chemistries (Bruce, Freunberger et al., 2012).

Battery Chemistry	Cell Voltage (V)	Theoretical Specific Energy (Wh/kg)	Theoretical Energy Density (Wh/l)
Li-ion	3.8	387	1015
Zn-air	1.65	1086	6091
Li-S	2.2	2567	2199
Li-O2 (non-aqueous)	3.0	3505	3436
Li-O2 (aqueous)	3.2	3582	2234

However, Li-O_2 batteries have unique complications that are currently hindering development. It has proven exceedingly difficult to produce consistent cells suitable for further research and characterisation. Therefore, the aim of this report is to determine and fully document an experimental method that focusses on reducing the inconsistencies during the Li-O_2 cell production process.

1.1 Electrode Materials

Within a metal-air battery, the metal functions as the anode and the cathode must consist of a highly mesoporous material combined with a polymer binder. In this case lithium was used for the anode and an activated carbon was used for the main cathode material.

1.1.1 Lithium Anode

Lithium is the metal of choice within metal-air batteries due primarily to the higher specific energies produced when compared to other metals like sodium, zinc and aluminium.

The half equation for lithium metal at the anode is as follows:

$$Li \rightleftharpoons Li^{+} + e^{-}$$

Equation 1 - Half equation for Lithium within Li-O_2 batteries.

The number of charge and discharge cycles within Li-O_2 cells is limited by dendrite formation across the solid-electrolyte interface layer (SEI). The dendrite formation is due to uneven current distribution across the anode surface because of the varying chemical composition due to the different reaction kinetics. Dendrite growth is problematic because it will typically lead to a short circuit occurring between the anode and cathode (Luntz and McCloskey, 2014).

1.1.2 Activated Carbon Cathode

Activated carbons are the most prolific cathode material within metal-air batteries. They can form a cathode with exceptionally high surface areas due to the inclusion of mesopores which form due to the nature of their physical properties. Pores are vital to allow for the unrestricted flow of oxygen through the cathode.

They are cheaper than other potential cathode materials (e.g. carbon nanotubes, carbon nanofibers) whilst retaining relatively good electrical properties (Zhang and Zhao, 2009).

Timcal Super C65 was used to form the cathode for the entirety of this project.

1.1.3 Kynar Flex Binder

The purpose of the binder is to ensure that the cathode has sufficient mechanical integrity to be self-supporting. For optimum performance the binder should be stable against radical-anion attack (Grande, Paillard et al., 2015).

In this case the binder used was Kynar Flex (2801).

1.2 Li-O_2 Battery Theory

The dominant electrochemical reactions that are known to occur within Li-O_2 batteries are commonly thought to be governed by the surface electrochemistry of the cell (Luntz and McCloskey, 2014). However, this matter is under contention with some sources instead claiming that O_2 reduction to Lithium Peroxide (Li_2O_2) occurs instead within the electrolyte solution and not at the surface of the cathode (Zhai, Wang et al., 2013). Thus, it is widely considered that the disproportionation reaction that occurs during discharge is not yet fully understood though more recently steps have been taken by (Johnson, Li et al., 2014) to produce a unified mechanism encompassing both of the current proposals.

The fundamental half equations agreed upon are found below. Please note that the forward direction for the following equations demonstrates the proposed mechanisms during cell discharge with the reverse reactions holding true for cell charging.

The electrochemical reaction that occurs at the anode is:

$$2Li \rightleftharpoons 2(Li^+ + e^-)$$

Equation 2 – Oxidation of Li at the anode.

The proposed surface electrochemistry mechanism at the cathode for oxygen reduction is shown below:

$$2(Li^+ + e^-) + O_2 \rightleftharpoons \mathrm{Li}_2O_2$$

Equation 3 – Formation mechanism of Li_2O_2 at the cathode.

However, some proposed mechanisms instead theorise that a Lithium Superoxide (LiO_2) intermediate is formed during the formation of lithium peroxide from the reduction of oxygen:

$$Li^+ + e^- + O_2 \rightleftharpoons \mathrm{Li}O_2$$

Equation 4 – Reduction of O_2 to form a LiO_2 intermediate.

This intermediate can then form lithium peroxide via one of two different mechanisms:

$$Li^+ + e^- + LiO_2 \rightleftharpoons \mathrm{Li}_2O_2$$

Equation 5 – Formation mechanism of Li_2O_2 at the cathode from the intermediate (1).

$$2LiO_2 \rightleftharpoons \mathrm{Li}_2O_2 + O_2$$

Equation 6 – Formation mechanism of Li_2O_2 at the cathode from the intermediate (2).

Research is still being performed on Li-O_2 cells to provide a universally accepted model for the electrochemical reactions that occur during cell discharge.

2 Experimental Method

As outlined briefly in the introduction the aim of this experiment was to produce cells demonstrating similar characteristics. Due to equipment and time limitations just 13 cells were able to be produced. The fundamental steps followed are outlined in the method below.

For cathode construction a mixture of 0.2 g of Timcal Super C65 and 0.05 g Kynar Flex binder (ratio of 80:20 activated carbon to binder) was produced, dissolved with an excess of acetone and heated and stirred magnetically until the desired viscosity was observable (in this case the solution had to successfully coat the magnetic stirrer). For cells 1 and 2, NMP was used to dissolve the mixture but it was found that during the latter coating process solvent evaporation occurred too rapidly and the mechanical integrity of the cathodes produced was poor, hence the use of acetone for cells 3 - 13.

After optimum viscosity had been achieved, the solution was coated onto a sheet of porous carbon paper at a thickness of approximately 100 μm (cells 1 and 2 had a thickness of 150 μm) using a draw down table and then completely dried under a vacuum at 120 °C. Cathode discs of diameter 12.5 mm were then punched out and transferred to the glove box.

A 1 M solution of $LiPF_6$ in TEGDME was prepared within a glove box to limit the amount of moisture contained within. Successful utilisation of the Karl Fischer titration method determined that the electrolyte had a moisture content of 1.4 ppm.

Complete Swagelok cell assembly was performed within a glove box. An exposed lithium disc of 12.5mm was cut out and placed on the solid cylinder within the Swagelok cell. A fibre glass separator (1 mm thickness) was fully saturated with the $LiPF_6$ in TEGDME (1 M) electrolyte and placed on top of the lithium disc. After this, the cathode disc was placed coating facing downwards on top of the fibre glass separator and then followed by an aluminium mesh current collector (approximately 12.5 mm thickness). Finally, the hollow, stainless steel top of the Swagelok was then added and then the whole cell was compressed and tightened. Care was taken throughout this process to ensure that the discs were in near perfect alignment to minimise the chance of short circuits occurring.

Following cell construction the Swagelok was transferred to an airtight glass containment vessel with external electrodes connected to the cell within. This vessel was securely sealed using Parafilm before it exited the glove box ready for the addition of oxygen.

The apparatus used to fill the glass vessel was initially purged with O_2 for 30 minutes to strip any moisture from the plastic tubing. The ports to the vessel were then opened to allow for the passage of O_2 across the cell. O2 flowed across the cell for 30 minutes before the vessel was securely sealed and connected to a Solartron 1400 Cell Test System for galvanostatic charge and discharge cycling.

The number of cells that could be produced within the allotted time was primarily limited by the number of glass testing vessels.

Table 2 – Swagelok Cells produced indicating which cell used which solvent.

Cell No.	Cathode Material		Composition Ratio	Solvent	Thickness
	Activated Carbon (AC)	Binder (B)	AC:B		(μm)
1 – 2	Timcal Super C65	Kynar Flex (2801)	80:20	NMP	150
3 – 13				Acetone	100

3 Method of Analysis

Galvanostatic charge and discharge cycling is the primary method used to characterise batteries. The characteristic determined for each cell in a bid to assess the consistency is the specific energy (Wh/kg) across the third and final (tenth) charge and discharge cycle. The third cycle was chosen as there was a communication error for the first two cycles between the Solartron and the computer software.

The cycling was performed using the MultiStat 1.1b program connected to a Solartron 1400 Cell test system. The C-rate used was determined via the mass of the activated carbon within the cathode. The safe operating potential range was 2 – 4.2 V based on values from literature for TEGDME (Li, Zhao et al., 2014).

The data produced from cycling was analysed using ZView 2.9b which is the accompanying graphical plotting tool to MultiStat 1.1b and Microsoft Excel. For this report, the software was used to produce graphs of Time (s) vs Potential (V). Data extracted from these plots provided values for current (I), potential (V) and time (t) which were used to successfully determine energy relative to activated carbon mass (m).

Specific energy was determined via:

$$E = \frac{IV\Delta t}{m}$$

Equation 7 – Specific energy calculation following galvanostatic charge and discharge cycling.

4 Results and Discussion

Of the 13 Swagelok cells produced just 10 were deemed suitable for analysis. Cell 1 failed to complete its sixth cycle due to experiencing a sudden voltage drop taking the voltage outside of the safe potential range. It is not certain why this drop occurred but it is thought that it may have been physically disturbed during testing. Because of this, Cell 2 was left unanalysed as it was the only other sample produced using NMP and of thickness 150 µm so the results would now of been incomparable. Cell 8 also failed to cycle due to an unknown short circuit being present within the glass containment vessel between the two electrodes. This caused the cell to fully discharge prior to cycling.

4.1 Discharge and Charge Cycles

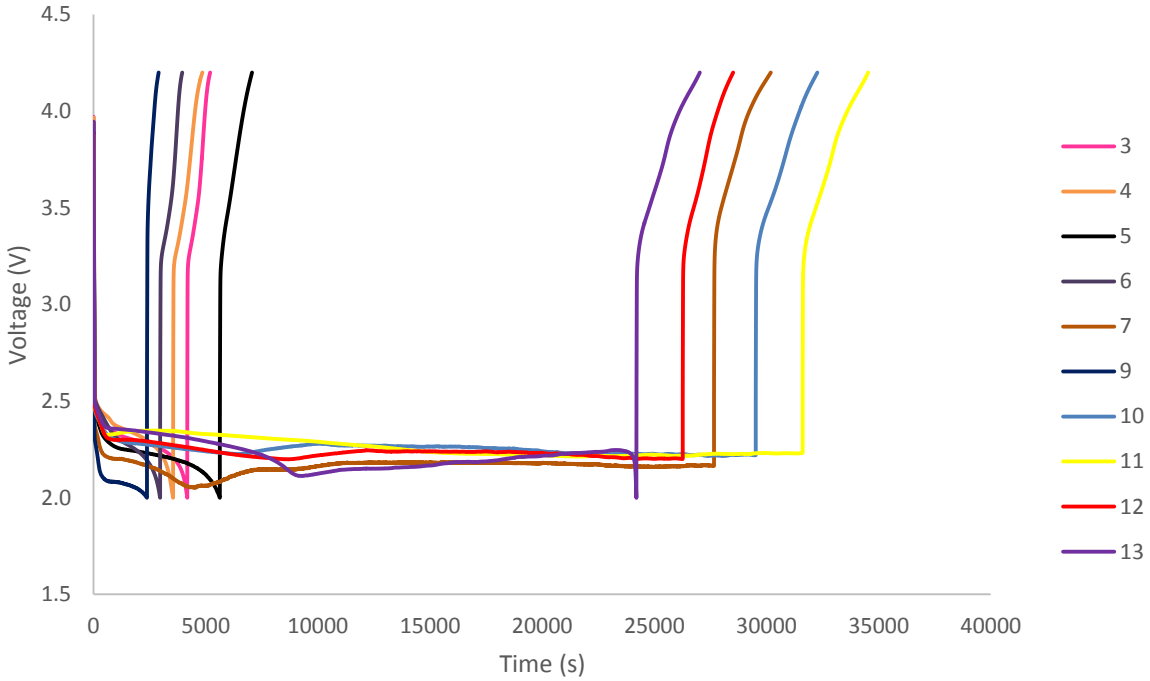

Figure 1 - Third discharge and charge cycle for each cell. The respective cell numbers are shown in the legend. There are clear differences in the time taken for discharge between the cells though the charging profiles are similar and finish over the same time period.

Figure 1 shows the third discharge and charge cycle for each cell that was analysable. The time has been offset to 0 s for each cycle. The time taken for complete discharge differs significantly from cell to cell though the time to taken to charge is approximately the same for each cell. Charging occurs rapidly which suggests that the Li metal is not being adequately broken down.

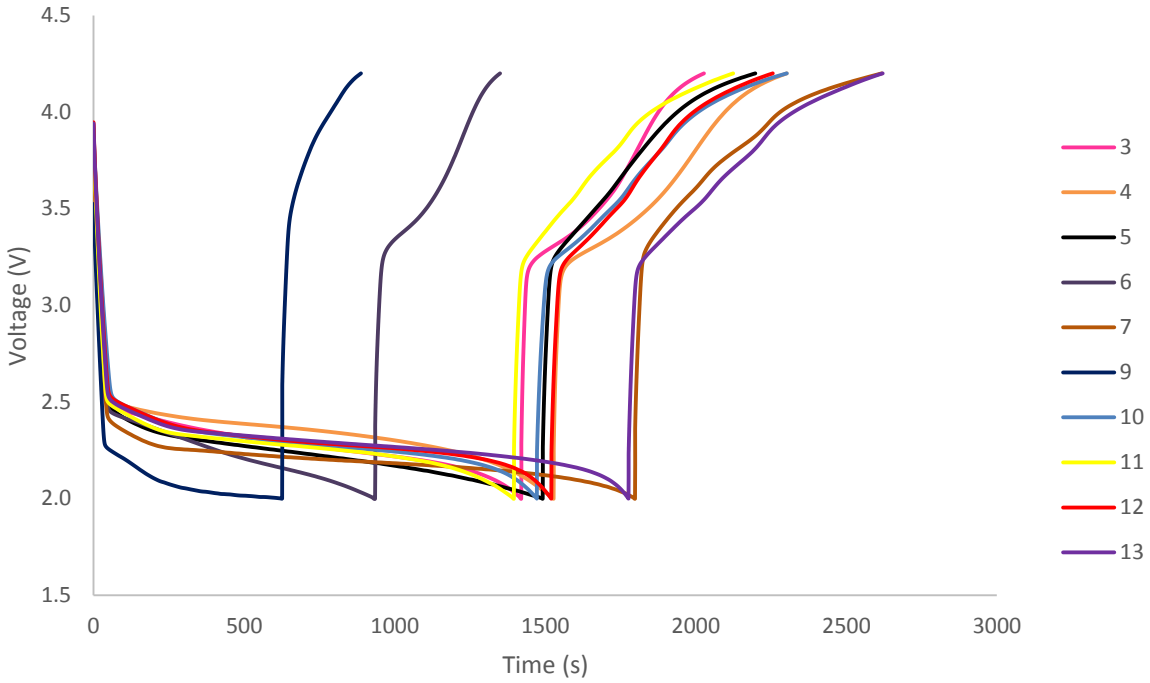

Figure 2 - Tenth discharge and charge cycle for each cell. The respective cell numbers are shown in the legend. There are clear differences in the time taken for discharge between the cells though the charging profiles are similar and finish over the same time period.

Figure 2 shows the tenth and final discharge and charge cycle for each cell. The time has been offset to 0 s for each cycle. As with the third discharge and charge profile there are vast differences between the times taken to fully discharge though the charging step occurs over relatively the same time period.

When the tenth cycle is compared to the third cycle it is clear that the battery is storing significantly less charge due to the time taken to discharge being almost an order of magnitude smaller for the tenth cycle than the third. This is clear evidence that the rechargeability of Li-O_2 cells is poor.

The discharge and charge profiles for both the third and tenth cycles demonstrate the inconsistencies of Li-O_2 cells as the time periods for each step varies significantly from cell to cell though the overall shapes are similar.

4.2 Specific Energy Comparison

Table 3 – Different energy values relative to mass for the third and tenth cycles for all cells and the standard deviation of the data.

Cell no.	Specific Energy (Wh/kg)			
	Discharge Cycle		Charge Cycle	
	3	10	3	10
3	-230.2	-78.3	89.4	53.2
4	-332.7	-144.3	192.8	114.0
5	-349.0	-93.5	149.6	74.4
6	-191.2	-59.6	100.5	42.5
7	-2163.1	-143.7	351.9	113.5
9	-161.4	-43.0	64.8	32.5
10	-2253.5	-115.3	351.3	105.2
11	-2264.2	-100.9	350.3	87.2
12	-2237.2	-133.9	323.4	104.9
13	-1653.8	-125.4	329.3	97.6
Standard Deviation	946.7	33.4	115.9	28.7
Standard Deviation of Highlighted Cells	259.0	12.3	12.4	7.3

The standard deviation indicates that the dispersion of the data across all the cells is vast. This reiterates that Li-O_2 cells are greatly inconsistent.

Cells 10 – 13 (highlighted in grey), the four most recently produced cells, show a standard deviation of 259 as opposed to a standard deviation of 946.7 for all cells for the third discharge. Whilst this value is still poor it potentially indicates that the consistency of the Li-O_2 cell production process improves with repetition.

The data in Table 3 also shows the diminished specific energies between the third and tenth cycles. This again demonstrates the poor rechargeability of Li-O_2 cells.

4.3 Lithium Anode Comparison

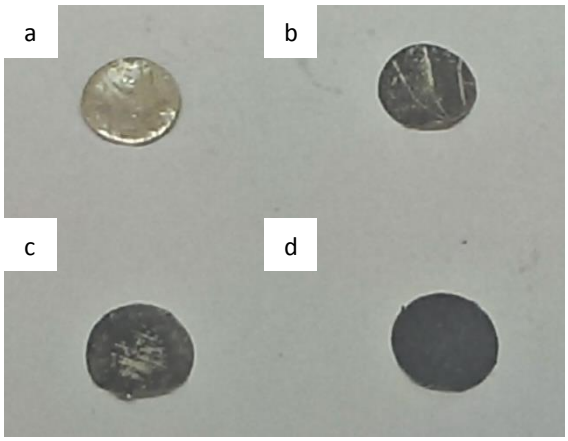

Figure 3 - Photo of Lithium anodes after different charge cycles. (a) Lithium Disc at 0 cycles. (b) Lithium disc after 3 cycles. (c) Lithium disc after 5 cycles. (d) Lithium disc after 10 cycles.

Figure 3 shows four lithium discs taken from Li-O_2 cells after a different number of cycles. (a) shows a lithium disc prior to cycling. The disc is completely silver and has a metallic shine. (b) and (c) show lithium discs after 3 and 5 cycles respectively. The discs now appear mostly matte black in colour though some silver colour is still present. (d) shows a lithium disc after 10 cycles. It is complete matte black with no silver colour present.

The matte black colour could be due to the formation of various Li compounds on the surface of the Li, such as lithium hydroxide, lithium carbonate and lithium nitride which are known to form when in the presence of moist air. It is thought that this black coating hinders the rechargeability of Li-O_2 cells.

5 Conclusion

The primary conclusion drawn from this study supports the original reasoning for this research which is that the current production method for Li-O_2 cells produces inconsistent cells. However, it was found that consistency was improved after repetition as the latter cells produced (10, 11, 12 and 13) showed similar discharge and charge profiles over approximately the same time period (see Figure 1 and Figure 2) and had a significantly smaller standard deviation (though still poor).

To further this research the sample size should be increased and causes for the inconsistencies should be investigated and identified.

6 Bibliography

Bruce, P. G., et al. (2012). Li-O-2 and Li-S batteries with high energy storage. *Nature Materials* 11(1) 19-29.

Cheng, F. and J. Chen (2012). Metal-air batteries: from oxygen reduction electrochemistry to cathode catalysts. *Chemical Society Reviews* 41(6) 2172-2192.

Christensen, J., et al. (2012). A Critical Review of Li/Air Batteries. *Journal of the Electrochemical Society* 159(2) R1-R30.

Grande, L., et al. (2015). The Lithium/Air Battery: Still an Emerging System or a Practical Reality? *Advanced Materials* 27(5) 784-800.

Johnson, L., et al. (2014). The role of LiO2 solubility in O-2 reduction in aprotic solvents and its consequences for Li-O-2 batteries. *Nature Chemistry* 6(12) 1091-1099.

Li, J., et al. (2014). An Effective Integrated Design for Enhanced Cathodes of Ni Foam-Supported Pt/Carbon Nanotubes for Li-O-2 Batteries. *Acs Applied Materials & Interfaces* 6(15) 12479-12485.

Luntz, A. C. and B. D. McCloskey (2014). Nonaqueous Li-Air Batteries: A Status Report. *Chemical Reviews* 114(23) 11721-11750.

Ottakam Thotiyl, M. M., et al. (2013). The carbon electrode in nonaqueous Li-O2 cells. *Journal of the American Chemical Society* 135(1) 494-500.

Peng, Z., et al. (2012). A Reversible and Higher-Rate Li-O-2 Battery. *Science* 337(6094) 563-566.

Soavi, F., S. Monaco and M. Mastragostino (2013). Catalyst-free porous carbon cathode and ionic liquid for high efficiency, rechargeable Li/O-2 battery. *Journal of Power Sources* 224 115-119.

Zhai, D., et al. (2013). Disproportionation in Li-O-2 Batteries Based on a Large Surface Area Carbon Cathode. *Journal of the American Chemical Society* 135(41) 15364-15372.

Zhang, L. L. and X. S. Zhao (2009). Carbon-based materials as supercapacitor electrodes. *Chemical Society Reviews* 38(9) 2520-2531.